Article

Research on the Cluster Hole Effect and Performance Testing of Air-Suction Quinoa Seed Metering Device

Xuan Zhao [1], Rongrong Liu [1,2], Fei Liu [1,*] , Hongbin Bai [1] and Wenxue Dong [1]

1   College of Mechanical and Electrical Engineering, Inner Mongolia Agricultural University, No. 306,
     Zhaowuda Road, Saihan District, Hohhot 010018, China; zhaoxuan@emails.imau.edu.cn (X.Z.);
     bhb81571@163.com (R.L.); bhb@emails.imau.edu.cn (H.B.); adong@emails.imau.edu.cn (W.D.)
2   Weichai Lovol Shangdong Axle &Transmission Co., Ltd., Linyi 273300, China
*   Correspondence: afei2208@imau.edu.cn; Tel.: +86-0471-4310717

Abstract: Quinoa and other small-seeded crops possess relatively diminutive seed diameters, rendering them highly susceptible to the influence of airflow. The seeding process is impacted by the Cluster Hole Effect, where seeds are unintentionally drawn into areas between the suction holes. This leads to multiple seeds being picked up at once, making it difficult to meet the precise seeding requirements for quinoa. To delve deeper into the mechanism of the cluster hole effects, this study focused on quinoa seeds as the primary research subject. This study analyzes the migration conditions of seed population suction and establishes an equation for seed suction considering the cluster hole effect. CFD methods were employed to analyze the impact of various vacuum chamber negative pressures, suction hole spacing, and suction hole quantities on the suction flow field. By combining simulation results with evaluation criteria such as the qualification rate of seeds per hole, the qualification rate of hole spacing, empty hole rate, and hole spacing coefficient of variation, single-factor experiments and Box–Behnken response surface experiments were conducted to analyze the effects of different factors and their interactions, ultimately determining an optimal parameter combination. The results indicate that with five suction holes, spaced at D11, a vacuum pressure of 1.2 kPa, and a rotation speed of 15 rpm, the seeding performance is optimal. The qualification rate of seeds per hole reaches 98.67%, the qualification rate of hole spacing is 96%, and the hole spacing coefficient of variation is 5.24%, meeting agricultural requirements.

Keywords: small-seeded crops; air-suction seed metering device; CFD; cluster hole effect; quinoa

1. Introduction

Quinoa, as a high-quality economic crop, not only possesses unique and rich nutritional value but is also adapted to poor, saline–alkali, arid, and cold arid regions [1]. Cultivating quinoa can not only increase farmers' income but also contribute to wind prevention, sand fixation, water conservation, and protection of cultivated land [2]. With the development of the quinoa industry, the demand for mechanized sowing of quinoa is increasing [3]. Existing quinoa sowing methods mainly include line sowing, hole sowing, and precision sowing. Among these, precision sowing has become the main research direction in quinoa sowing due to its stable number of seeds per hole and seed-saving advantages [4]. Existing precision seed metering devices are generally divided into mechanical and pneumatic types [5,6]. Mechanical precision seed metering devices, which can damage seeds and struggle to control the number of seeds per hole, do not meet the precision sowing needs of small-grain crops [7,8]. Air-suction seed metering devices, on the other hand, due to their low seed damage rate and ability to precisely sow different numbers of seeds per hole, are widely used in the sowing of small-grain crops [9,10].

Seeds can be classified into two categories based on their average grain size: large and small [11]. For large-grain seeds, such as soybeans and corn, single-grain precision

seed metering devices are commonly used. Research in this area primarily focuses on various aspects, including hole structure [12], seed-clearing devices [13], working negative pressure [14], working speed [15], and suction posture [16]. Significant achievements have been made in both theoretical research and model development for precision seed metering devices designed for large-grain seeds [17–19]. In contrast, small-grain seeds, which have an average diameter of less than 3 mm, are lighter, more susceptible to airflow, and prone to breakage. This makes seed picking and clearing more challenging with traditional air-suction seed metering devices [20].
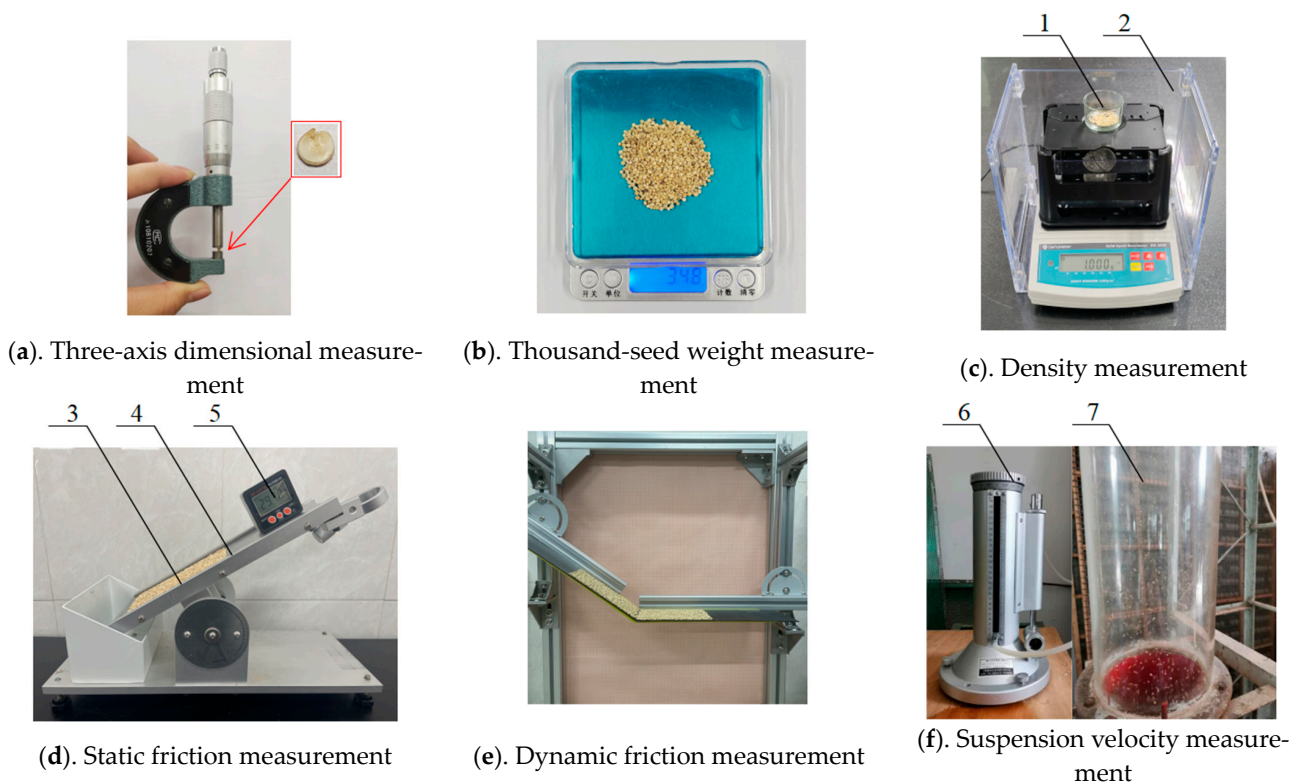
Consequently, many scholars have designed seed metering devices suitable for small-grain crops, adapting the technology used for large-grain air-suction devices [21]. Li et al. [22] investigated the impact of the spoon structure on the seed count per hole in millet. Liao et al. [23] identified key factors affecting the stability of seed picking for small-grain seeds, such as rapeseed and cabbage, which are nearly spherical in shape. Li et al. [24] explored how machine working speed affects the precision seed metering devices' qualification index for rapeseed. Li et al. [25] designed a dual-row pneumatic precision seed metering device for small bok choy, enhancing the seeding efficiency and precision. Xu et al. [26] used CFD-DEM coupling to analyze the microscale interactions between rapeseed and airflow. Anton et al. [27] explored the impact of different components inside the seed metering device on the distribution of airflow in the seed box. Research on seed metering devices for both large and small grain sizes has primarily focused on single-grain precision in picking, clearing, and sowing. There has been less exploration into multi-grain precision picking.

Quinoa seeds, distinct from other small-grain crops sown with single-seed precision, are frequently sown using a multi-seed precision hole sowing method. An insufficiency in the number of seeds per hole can adversely impact the emergence period and rate, subsequently resulting in spatial discontinuities and irregularities in crop rows. In contrast, an excess of seeds per hole precipitates a scenario of acute competition for essential growth resources, such as sunlight, water, and nutrients, thereby inducing a state of overcrowding among the seedlings [28,29]. To mitigate the variability inherent in multi-seed air-suction precision seed metering devices and to counteract the issue of controlling the number of seeds per hole by the cluster hole effect, this study embarks on a theoretical examination of the underlying causes of the hole clustering effect. Leveraging CFD for numerical simulation, this research identifies the principal factors contributing to the hole clustering effect. Through these insights, an enhancement in the design of the seed disk is proposed, facilitating the achievement of accurate multi-seed sowing for quinoa, thus ensuring the air-suction quinoa precision seed metering device's reliability and efficiency.

2. Materials and Methods

2.1. Parameter Measurement

For the experiment, "Mengli No. 1" quinoa seeds were selected. The three-axis dimensions of the seeds were measured using a micrometer (Figure 1a). The thousand-seed weight was measured using an electronic scale (Figure 1b). The seed density was measured using a DH-300X solid–liquid dual-use density meter (Figure 1c). The static friction coefficient of the seeds was determined using an inclinometer (Figure 1d). The dynamic friction coefficient of the seeds was measured using a custom-built dynamic friction coefficient testing platform (Figure 1e). The seed suspension velocity was measured using a straight tube airflow critical speed detector (Figure 1f). The test results are shown in Table 1.

(**a**). Three-axis dimensional measurement

(**b**). Thousand-seed weight measurement

(**c**). Density measurement

(**d**). Static friction measurement

(**e**). Dynamic friction measurement


(**f**). Suspension velocity measurement

Figure 1. Measurement of physical parameters: 1. The quinoa seeds to be tested. 2. Solid–liquid Densimeter DH-300X 3. Seed bonding plate. 4. Slope instrument. 5. Digital display inclinometer. 6. Micromanometer. 7. Seed suspension tube.

Table 1. Summary of physical characteristics of quinoa seeds.

Parameter		Value
Length (mm)		2.289
Width (mm)		2.142
Thickness (mm)		1.274
Sphericity		0.805
Thousand-grain mass/g		3.6
Density/(kg·m^{-3})		1100
Suspension velocity (m·s^{-1})		4.46~5.67
Static friction	Seed–Seed	0.62
	Seed–PLA	0.55
Dynamic friction	Seed–Seed	0.27
	Seed–PLA	0.25

2.2. Structure and Working Principle of Seed Metering Device

The overall structure of the experimental seed planter includes a seed box, seed suction foil, stirring plate, seed metering plate body, air guide tube, and air chamber, as depicted in Figure 2. When the planter operates, the stirring plate agitates the stationary seeds in the seed box, enhancing their flow and moving them into the seed-suctioning area. In this area, seeds are adsorbed onto the seed suction foil due to negative pressure and rotate with the seed metering plate body. After rotating a specific angle, the adsorbed seeds detach from the population and enter the seed-cleaning area. Seeds that are not stably suctioned to the metering plate fall back into the seed box. Those stably suctioned on the plate pass through the seed-carrying area to the seed-unloading area. Here, as the negative pressure ceases, the seeds detach from the plate and fall into the guide tube, completing one cycle of the seeding process.
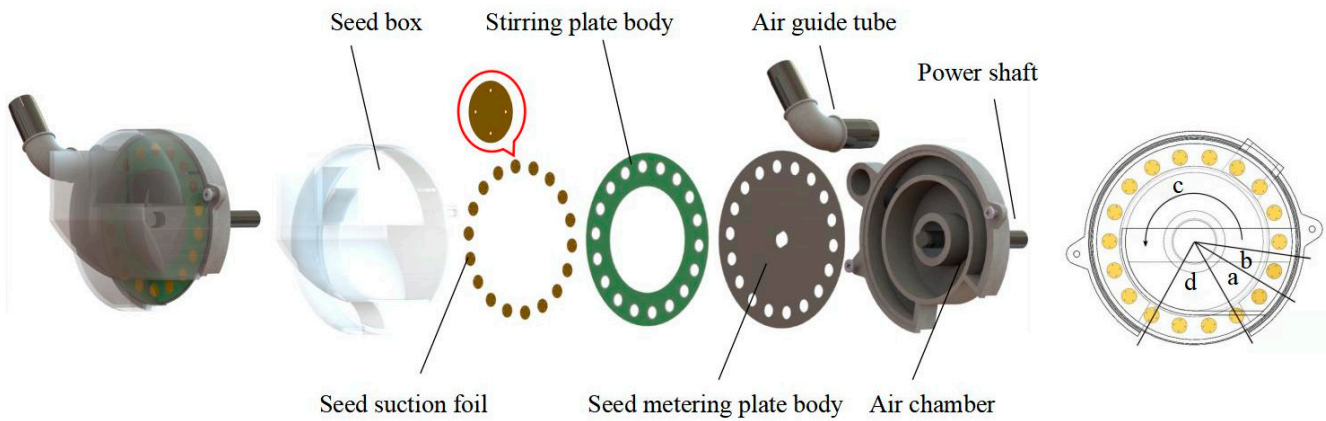
Figure 2. Structure diagram of seed metering device: a. Seed-filling area. b. Seed-suctioning area c. Seed-carrying area. d. Seed-unloading area.

2.3. Cluster Hole Effect Analysis

2.3.1. Analysis of Seed Suctioning Stability

To explore the key factors affecting stable seed adhesion and determine the critical adhesion conditions, further analysis of the forces acting on the seeding process is required. During the operation of the seed metering device, it is assumed that a single suction hole only adheres to a single seed, and all external forces act on the centroid of the seed. Taking the centroid of the seed as the origin o, the direction of rotation of the seed disc is denoted as the o_i direction, the direction from the centroid of the seed pointing towards the center of the seed disc is denoted as the o_j direction, and the direction perpendicular to the plane of the seed disc is denoted as the o_k direction, establishing a natural coordinate system, as shown in Figure 3. According to the principle of D'Alembert, the equilibrium equation is formulated as in Equation (1).
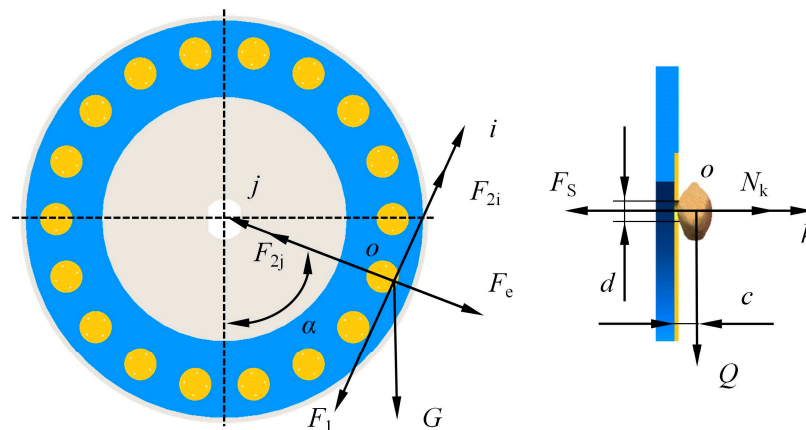
Figure 3. Analysis of seed suctioning stability: F_{2i} is the frictional force component in the o_i direction between the seed and the seed suction foil, F_{2j} is the frictional force component in the o_j direction between the seed and the seed suction foil, F_1 is the frictional force between the seeds, assuming its direction is in the negative o_i direction, F_e is the centrifugal force, F_S is the adhesive force of suction holes on seeds in the airflow field, N_k is the constraining force of seed suction holes on seeds, d is the diameter of the seed suction hole, m is the mass of the seed, f_1 is the friction coefficient between seeds. f_2 is the friction coefficient between seeds and the seed suction foil. ω is the angular velocity of the seeding disc, R is the rotational radius of the suction hole center in the seeding disc, c is the spacing from the seed center of mass to the seeding disc, j is the normal direction of the seed metering plate's rotation, i is the tangential direction of the seed metering plate's rotation, and k is the secondary normal direction perpendicular to the seed metering plate.

$$\begin{cases} \sum F_i = 0 \Rightarrow F_{2i} - F_1 - G\sin\alpha = 0 \\ \sum F_j = 0 \Rightarrow F_{2j} - F_e - G\sin\alpha = 0 \\ \sum F_k = 0 \Rightarrow F_s - N_k = 0 \\ F_s = PS \\ F_1 = mgf_1 \\ F_2 = \sqrt{F_{2i}^2 + F_{2j}^2} = N_k f_2 \\ F_e = m\omega^2 R \end{cases} \tag{1}$$

Seed stabilization suction should satisfy Equation (2).

$$(F_S - N_k)\frac{d}{2} \geq Qc \tag{2}$$

When $N_k = 0$, the seed suction critical state is satisfied; at this time, the minimum critical suction force is shown in Equation (3).

$$F_s = \frac{2c}{d}\sqrt{F_e^2 + G^2 + 2GF_e\cos\alpha + F_1^2 + 2F_1\sqrt{G^2 + F_e^2 + 2GF_e\cos\alpha}\cos\beta} \tag{3}$$

Ideally, the seed is also influenced by natural and external environments during the operation of the seed planter. Considering the reliability coefficient of seed suction (K_1), the working stability and reliability coefficient (K_2), and the water content effect coefficient of the seed (K_3) [30], and taking the maximum limit conditions of $\cos\alpha = 1$ and $\cos\beta = 1$, then seeds are adsorbed when the critical suction pressure is reached, as in Equation (4).

$$P \geq \frac{2cK_1K_2K_3}{Sd}(F_e + G + F_1) \tag{4}$$

In the suction process, according to Bernoulli's equation, as in Equation (5), the seed is in the flow field with a certain flow rate; at this time, the seed is subjected to the force of the airflow, which is related to the airflow rate.

$$\Delta P = \frac{1}{2}\rho\left(v^2 - v_0^2\right) \tag{5}$$

where ΔP is the pressure difference across the suction holes; v is the air flow velocity at the suction hole of the air chamber; v_0 is the air flow velocity of the seed box, where $v_0 = 0$; and ρ is the air density.

Assuming that quinoa seeds are homogeneous spheres, Equations (4) and (5) give the theoretical sorption flow rate as in Equation (6).

$$v \geq \sqrt{\frac{4cK_1K_2K_3}{S\rho d}(F_e + G + F_1)} \tag{6}$$

Under standard conditions, the air density ρ is 1.29 kg·m^{-3}; the equivalent diameter of quinoa Φ is 1.64 mm; the thousand-seed weight of the seeds is 3.6 g; the dynamic friction coefficient between populations is $f_1 = 0.26$; the reliability coefficient for seed suction, the external condition influence coefficient, and the water content effect coefficient of the seeds are taken as $K_1 = 2$, $K_2 = 1.8$, $K_3 = 1.1$, respectively; the diameter of the suction hole d is 0.8 mm; the rotation speed of the seed metering plate is set at 15 rpm; and the rotation radius R from the center of the suction hole to the seed metering plate is taken as 82.5 mm. The theoretical calculations indicate that when the suction area is $S = \pi d^2/4$, and the airflow velocity acting on the seeds reaches 30.22 m·s^{-1}, it can satisfy the stable suction of the seeds. Considering the experimental error during the measurement of seed physical properties and the complex environment during the seed suction process, a higher negative pressure flow rate should be adopted in practice to meet the operational requirements.

2.3.2. Analysis of Cluster Hole Effect

In order to further analyze the key factors affecting the cluster hole effect, a single seed between suction holes was subjected to mechanical analysis. The seeds are assumed to be spherical rigid bodies with a constant pressure region within the gas chamber. According to the forces acting on seed particles in fluid, the seed is typically subjected to a combination of multiple forces. However, in practice, since the seed does not generate high acceleration or high-speed rotation, the additional mass force, Basset force, Magnus force, and Saffman force can be neglected [31,32]. The simplified force analysis of the seed when a single suction hole is applied is illustrated in Figure 4.
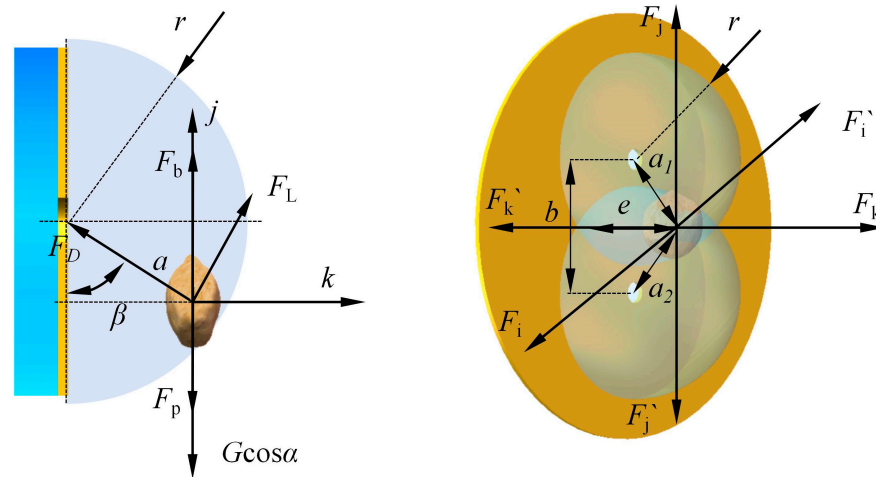
Figure 4. Analysis of cluster hole effect: F_D is the perturbation resistance of the suction hole airflow to the seed, F_L is the perturbation lift of the suction hole airflow to the seed, F_p is the pressure gradient force, F_b is the buoyancy force, N_k is the support force, G is the gravitational force, b is the spacing between the centers of the two suction holes, c is the spacing of the seed center of mass from the suction sheet, a is the spacing of the seed center of mass from the suction holes, β is the angle of the line between the center of the suction holes and the center of mass of the seeds to the plane of the suction sheet, and r is the critical region of action of the suction holes maximum radius. F_i', F_i', F_j', F_j', F_k', F_k' are the forces on the seed along the i-axis, the j-axis, and the k-axis, a_1 is the spacing of the seed from the upper suction hole, a_2 is the spacing of the seed from the lower suction hole, and e is the perpendicular spacing of the seed from the suction sheet.

According to the principle, the fluid-structure interaction dynamics can be listed in Equation (7).

$$G \cos \alpha - F_D \cos \beta - F_L - F_b + F_p = 0 \tag{7}$$

Calculate Equation (7) to obtain Equation (8).

$$\rho_p g V_p \cos \alpha - \frac{1}{2} \rho C_d A_s v^2 \cos \beta - \frac{1}{2} \rho C_L A_s v^2 \sin \beta - \rho g V_p - V_p \nabla p = 0 \tag{8}$$

where C_d is the disturbance drag coefficient; As is the seed windward area; v is the airflow velocity; C_L is the lift coefficient; V_p is the seed volume; ∇p is the pressure gradient force; ρ is the fluid density; and ρ_p is the seed density.

Assuming the range of action of the airflow forms a sphere, the spherical surface, centered at the sphere's center and at a spacing r, possesses a uniform airflow rate. Due to the influence of the seed-absorbing sheet, the actual suction area is reduced to a hemisphere, the area of which is delineated in Equation (9).

$$A = 2\pi r^2 \tag{9}$$

The velocity of any equivalent surface airflow in the action sphere can then be expressed by Equation (10) [33].

$$v = \frac{d^2}{8r^2}\sqrt{\frac{2k}{k-1}RT_e\left[1 - \left(\frac{p_i}{p_e}\right)^{\frac{k-1}{k}}\right]}$$

(10)

where R is the gas constant; T is the absolute temperature; k is the heat fusion ratio; p_e is the atmospheric pressure; and p_i is the pressure at the suction hole.

Substituting Equation (10) into Equation (8) yields the theoretical suction radius r, as presented in Equation (11).

$$r = \sqrt[4]{\frac{3\rho d^4(C_d\cos\beta + C_L\sin\beta)kRT_e\left[1 - \left(\frac{p_i}{p_e}\right)^{\frac{k-1}{k}}\right]}{128\pi^2\phi(\Delta\rho g - \nabla p)(k-1)}}$$

(11)

Building upon the analysis of the single holes-absorbing effect, the cluster hole effect was further examined, as depicted in Figure 4. Neglecting the effect of the seed's profile volume and assuming that the flow field forces act upon the seed's center of mass, the airflow velocity for varying seed positions can be derived from Equations (10) and (11), as indicated in Equation (12). It is observed that, under the influence of the interacting airflow field, the velocity of the airflow within the space is dependent upon the spacing between the seeds and the suction holes, the diameter of the suction holes, the spacing between the holes, and the magnitude of the pressure differential.

$$\begin{cases} v = \frac{d^2}{8a^2}\sqrt{\frac{2kRT_e}{k-1}\left[1 - \left(\frac{p_i}{p_e}\right)^{\frac{k-1}{k}}\right]} & b > 2r \\ v = \sqrt{\frac{d^2\left(a_1^2 + a_2^2\right)kRT_e}{32a_1^2a_2^2(k-1)}\left[1 - \left(\frac{p_i}{p_e}\right)^{\frac{k-1}{k}}\right]} & b \le 2r \cap \begin{cases} a_1 < \sqrt{r^2 - e^2} \\ a_2 < \sqrt{r^2 - e^2} \end{cases} \end{cases}$$

(12)

2.4. CFD Simulation Test

This study uses ANSYS Fluent to analyze the airflow at the suction holes in different regions of the seed metering device in a stationary state. This analysis aims to further investigate the changes in airflow at the suction holes of the seed metering device. In the flow field simulation analysis, emphasis is placed primarily on the internal flow field region, necessitating the construction of an internal fluid region model [34]. By simplifying the seed discharger model and extracting the fluid domain, the model of the fluid domain is obtained, as illustrated in Figure 5a. Through Fluent meshing, the Poly-Hexcore volume mesh generation method was used to divide the fluid domain into grids (Figure 5b).

A grid independence verification was performed on the model, with the monitored region being the mid-plane between the two ends of the seed suction foil. Considering both calculation accuracy and efficiency, Grid 3 was selected for numerical simulation (Table 2). Auto Node Move was used to optimize the grid model to ensure convergence of the results. Grid quality monitoring indicated a maximum skewness of 0.75 and a minimum orthogonal quality of 0.36, meeting the computational requirements. To further ensure consistency between the simulation results and the actual results, an HT-1890 digital manometer was used to measure the negative pressure at a single suction hole on a macro level, which was then used to correct the simulation parameters. The k-epsilon turbulence Standard model was selected for this study, with air as the material property for the fluid domain. The outlet pressure was set to different negative pressure levels, the inlet pressure was set to 0 kPa, and the remaining boundary conditions were set as walls for the simulation.
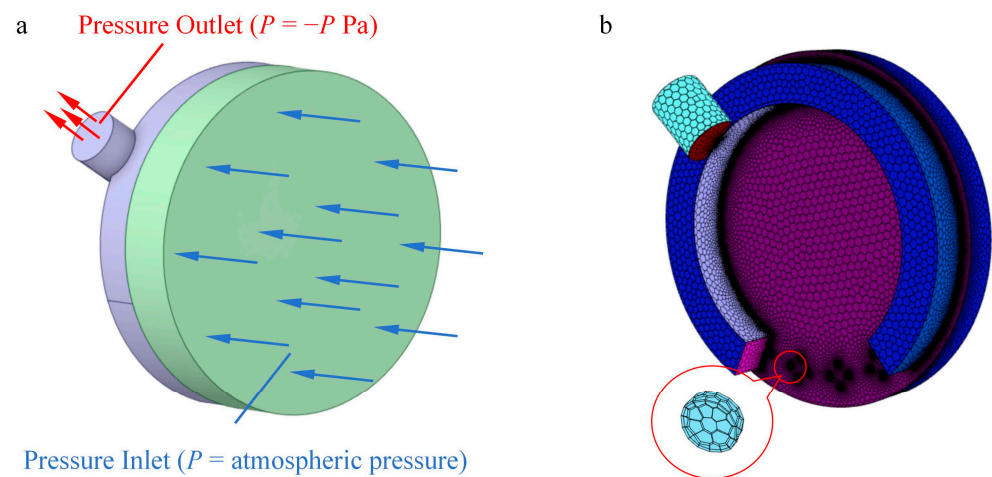
Figure 5. Fluid simulation model. (**a**). Fluid domain (**b**). Mesh.

Table 2. Grid independence verification.

Parameters	Total Number of Cells	Airflow Velocity in the Measurement Point Region
1	4.33×10^5	54.6
2	7.14×10^5	51.1
3	1.19×10^6	50.3
4	1.45×10^6	50.2
5	2.02×10^6	49.9

2.5. Seeding Performance Test

"Meng quinoa No. 1" seeds were selected for experimental research, utilizing the JPS-12 computer vision seed metering device test bench (Figure 6). The experiment was conducted in March 2024.
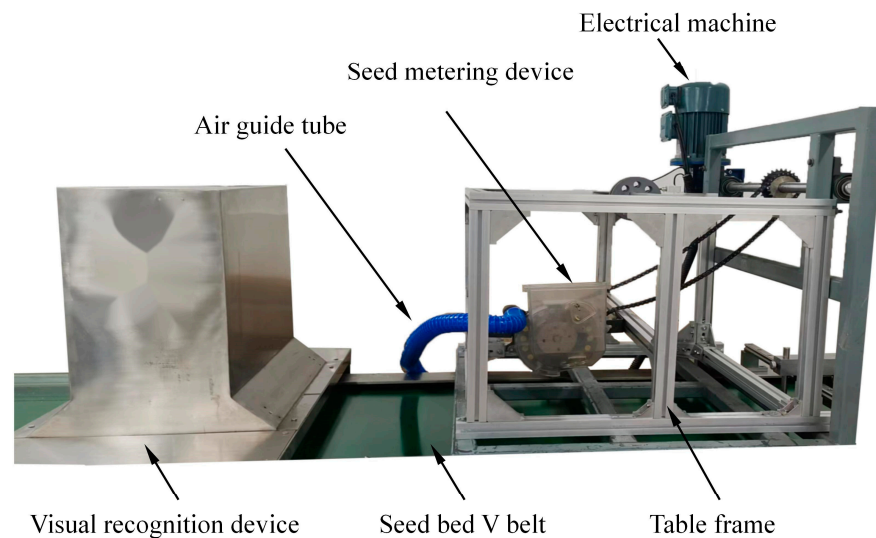
Figure 6. JPS-12 computer vision seed metering device test bench.

Adhering to industry standards NY/T 987-2006 for film-laying hole sower operation quality and NY/1823-2009 for greenhouse vegetable hole-disk precision seeder technical conditions, and incorporating simulation test results, this study conducted experiments focusing on the number of suction holes, the suction hole spacing, and the negative pressure. Based on the preliminary experiment results, a single-factor experiment (Table 3) and a BB response surface experiment (Table 4) were conducted.

Table 3. Single-factor experiments.

Level Code	Factors		
	Number of Suction Holes *A*	**Suction Hole Spacing *B***	**Negative Pressure *C***
1	3	D3	0.6
2	4	D5	0.8
3	5	D7	1
4	6	D9	1.2
5		D11	1.4

Note: D3 stands for a center distance of 3 mm, while D5–D11, respectively, represent center distances of 5–11 mm.

**Table 4.** BB response surface experiment.

Level Code	Factors		
	Number of Suction Holes *A*	**Suction Hole Spacing *B***	**Negative Pressure *C***
1	3	D7	0.8
0	4	D9	1
−1	5	D11	1.2

3. Results

3.1. Simulation Results Analysis

3.1.1. Effect of Different Positions on the Flow Field

The average airflow velocity across the end face of the seed suction foil was analyzed to investigate the airflow distribution across various locations within the air chamber. Owing to the small diameter of the seed suction holes, which hindered easy observation, this study assigned numbers to the seed suction holes on the 18 seed suction tablets. Specifically, seed suction holes No. 1–14 were situated in the negative pressure area, while holes No. 15–18 were located in the non-negative pressure area, as depicted in Figure 7a. Using a 4-hole seed discharge disk, with a negative pressure of −3 kPa and a hole spacing of 11 mm as an example, average airflow velocity values at the end faces of the seed suction holes in different locations were recorded, as illustrated in Figure 7b. Under identical air chamber conditions, the variance in average airflow velocity values among different positions was minimal, showing slight fluctuations within a certain range. Consequently, any suction hole position could be chosen for analyzing the cluster hole effect.

(**a**)

(**b**)
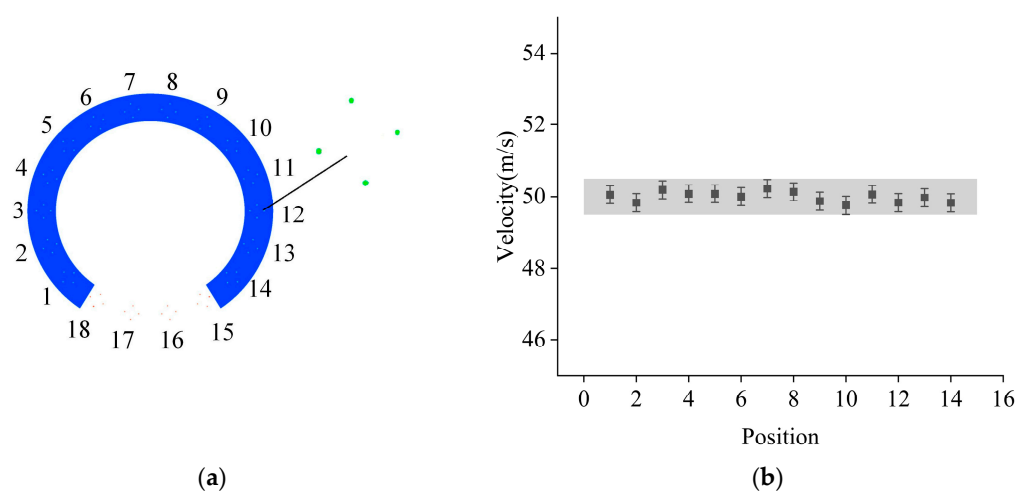
Figure 7. Effect of different positions on the flow field. (**a**). Distribution location; (**b**). Average airflow velocity.

3.1.2. Effect of Suction Hole Spacing on the Flow Field

To facilitate the analysis of flow field changes influenced by various parameters, a straight line through the center of the suction hole is intercepted in the 3D model. This line lies on the end face of the seed suction foil, as illustrated in Figure 8.

Figure 8. Schematic diagram of suction hole spacing.

The variation in the airflow field relative to the spacing between suction holes was analyzed, with the spacing serving as a variable. By extracting the airflow data along the straight line on the end face, the variation in the suction area as a function of suction hole spacing was charted, as shown in Figure 9. The region exhibiting suction near the seed-sucking holes was approximated as a circle. By extracting both the actual perturbed airflow velocity (seed suspension velocity) and the theoretical stabilized suction airflow velocity from the intersection points of the curves, the area of the region adjacent to the suction hole—exhibiting both suction and perturbation effects on quinoa seeds—was calculated, with the results depicted in Figure 10. During the seed suction process, the suction area initially decreases with the gradual increase in the spacing between suction holes; when this spacing exceeds 7 mm, the extent of the suction area fluctuates around a specific value.
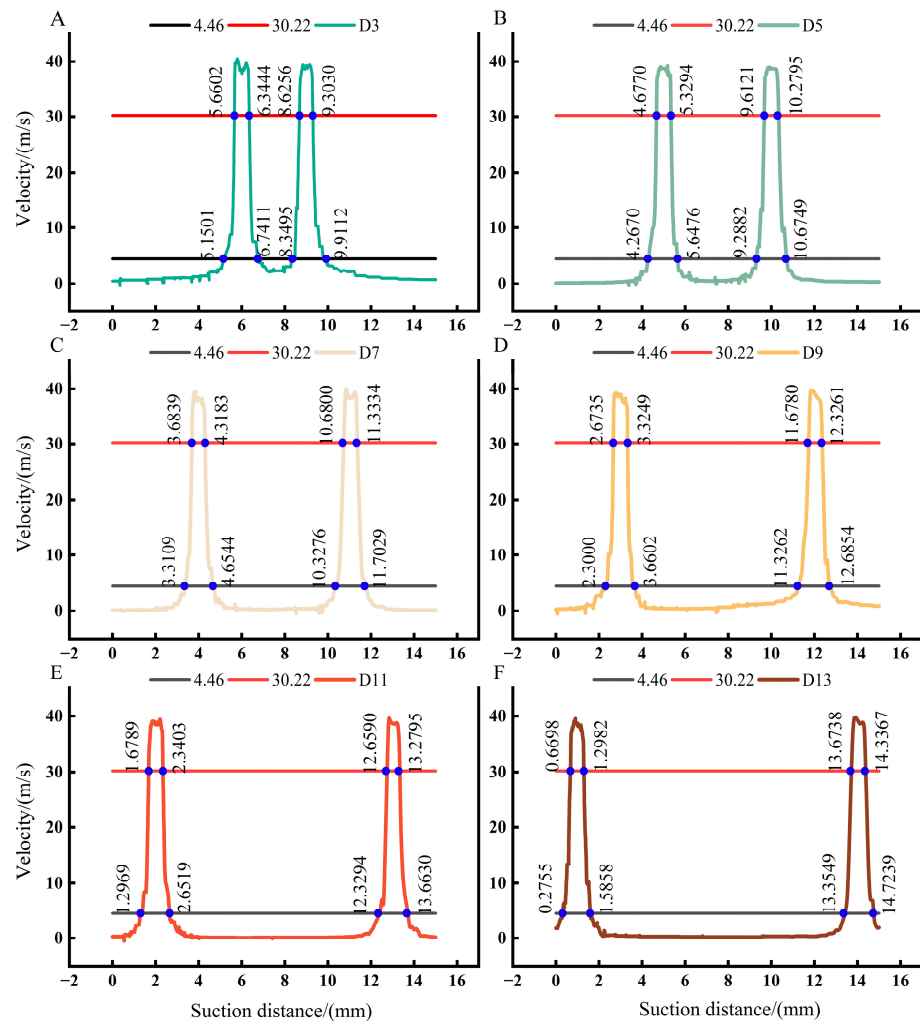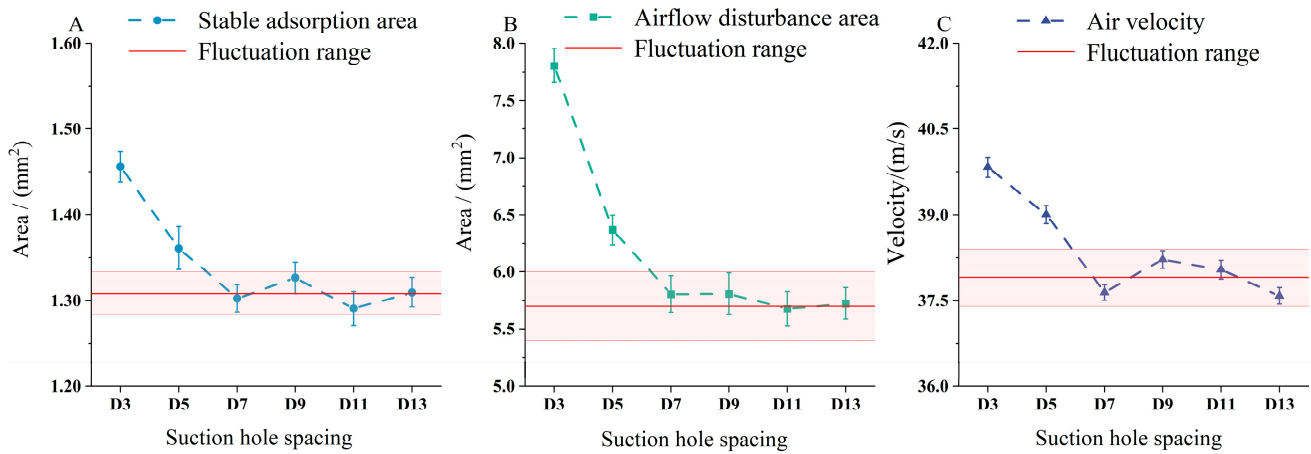

Figure 9. Effect of the suction hole spacing on the suction region. (**A**). D3; (**B**). D5; (**C**). D7; (**D**). D9; (**E**). D11; (**F**). D13.

Figure 10. Results of suction hole spacing analysis. (**A**). Stable adsorption area; (**B**). Airflow disturbance area; (**C**). Air velocity.
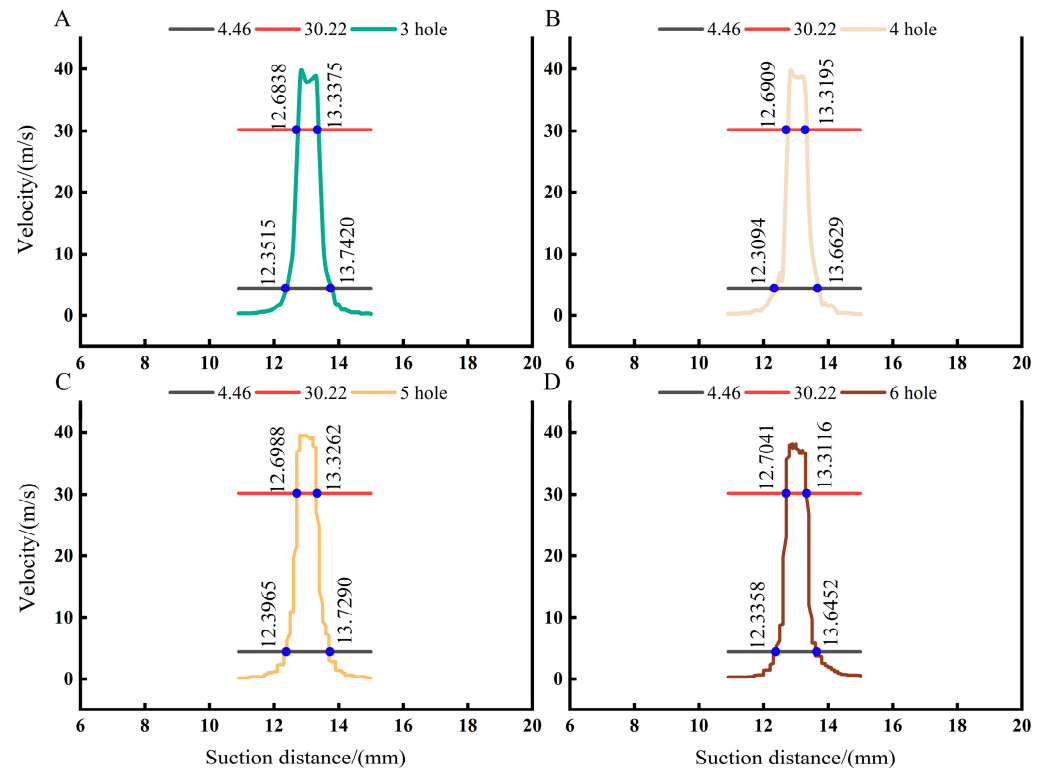
3.1.3. Effect of the Number of Suction Holes on the Flow Field

To facilitate the analysis, the study focuses solely on the flow field change rule for a single suction hole under various numbers of suction holes. The distribution spacing of suction holes is designated as D11 to mitigate the impact of airflow changes caused by overly proximal distribution spacings of suction holes. The distribution of the number of suction holes is depicted in Figure 11.

(**a**). Three holes   (**b**). Four holes   (**c**). Five holes   (**d**). Six holes
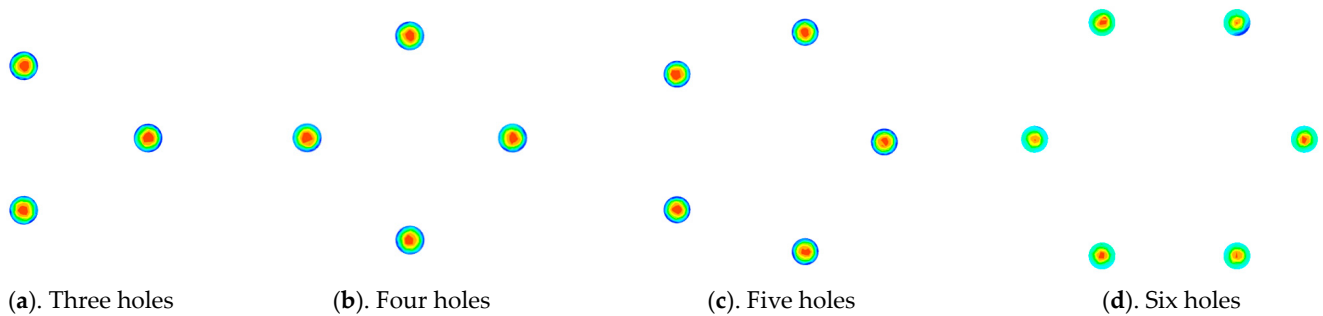
Figure 11. Different number of suction holes.

Using the number of suction holes as a variable, the study analyzed the airflow field's change rule relative to the number of suction holes. Airflow data along the end face straight line was extracted to illustrate the variation in the suction region with the number of suction holes, as shown in Figure 12. The area adjacent to the suction holes, calculated to both adsorb and disturb the quinoa seeds, is presented in Figure 13. During the seed suction process, as the number of suction holes increases, the area of single suction holes with adsorbed seeds decreases; however, this range of change is minor and meets the condition for the minimum critical suction of seeds. The velocity of airflow at the suction holes decreases with an increase in the number of suction holes, but the extent of this change is limited, indicating that the number of suction holes does not significantly affect the velocity of airflow at the suction holes.

Figure 12. Effect of the number of suction holes on the flow rate. (**A**). 3 holes; (**B**). 4 holes; (**C**). 5 holes; (**D**). 6 holes.
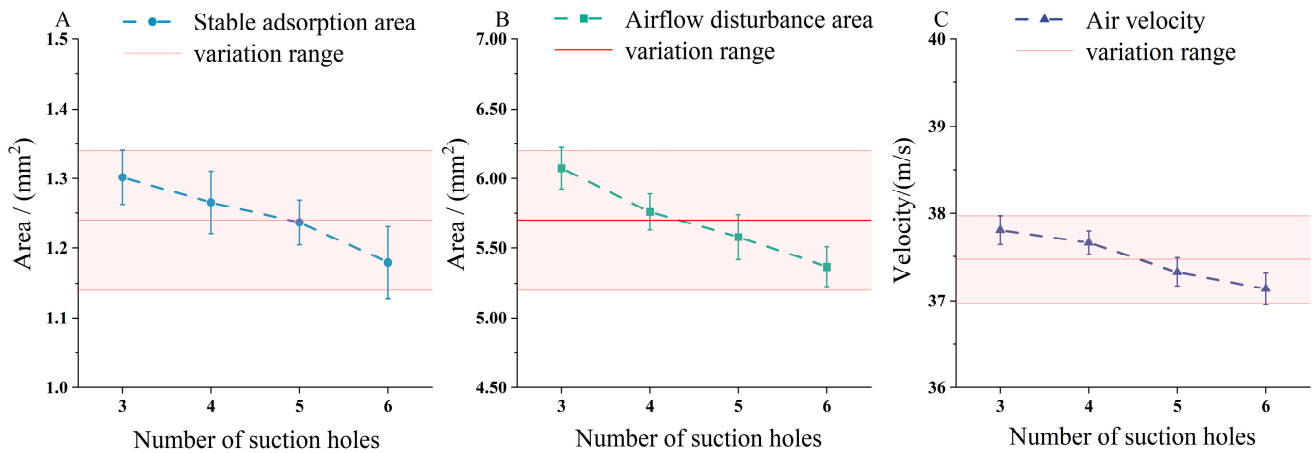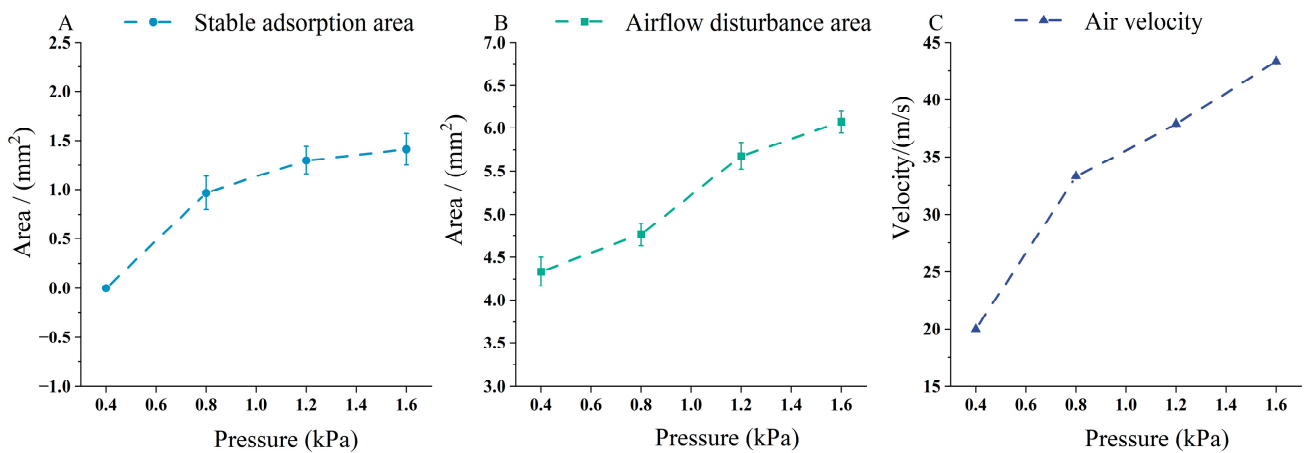

Figure 13. Results of the number of suction holes analysis. (**A**). Stable adsorption area; (**B**). Airflow disturbance area; (**C**). Air velocity.

3.1.4. Effect of Negative Pressure on the Flow Field

Using the negative pressure within the air chamber as a variable, the study analyzes the change rule of the airflow field in relation to the negative pressure of the air chamber. The variation of the suction region with the negative pressure of the air chamber was illustrated, as depicted in Figure 14. The area adjacent to the suction hole, encompassing both the suction and perturbation regions for quinoa seeds, is calculated and shown in Figure 15.
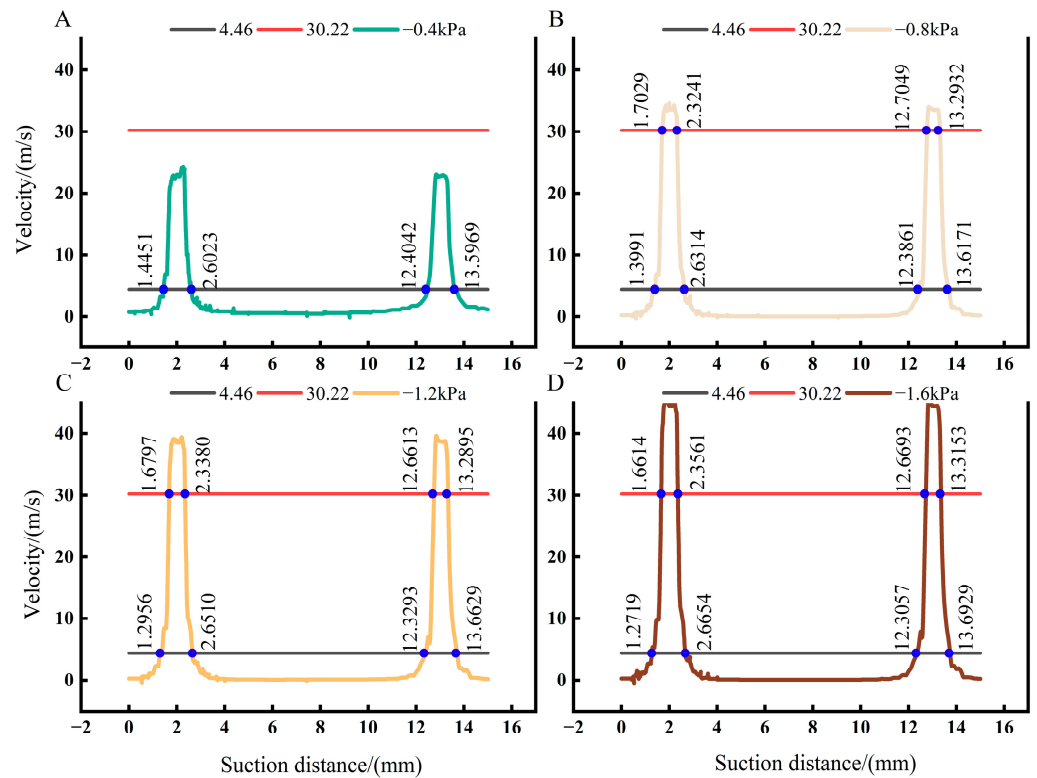
Figure 14. Effect of negative air chamber pressure on flow rate. (**A**). −0.4 kPa; (**B**). −0.8 kPa; (**C**). −1.2 kPa; (**D**). −1.4 kPa.


Figure 15. Results of negative air chamber pressure analysis. (**A**). Stable adsorption area; (**B**). Airflow disturbance area; (**C**). Air velocity.

In the process of seed suction, the suction region initially increases with a gradual rise in negative pressure; similarly, the velocity of the airflow at the suction hole also increases with the enhancement of negative pressure. When the negative pressure at the suction hole is −0.4 kPa, the flow rate at the suction hole fails to meet the conditions for seed suction, yet it can facilitate seed perturbation. However, when the negative pressure at the suction hole reaches −0.8 kPa, the flow rate at the suction hole essentially satisfies the critical conditions for seed suction. This indicates that the magnitude of the negative pressure is a critical factor influencing the stable suction of seeds.

3.2. Results Analysis of the Single-Factor Test

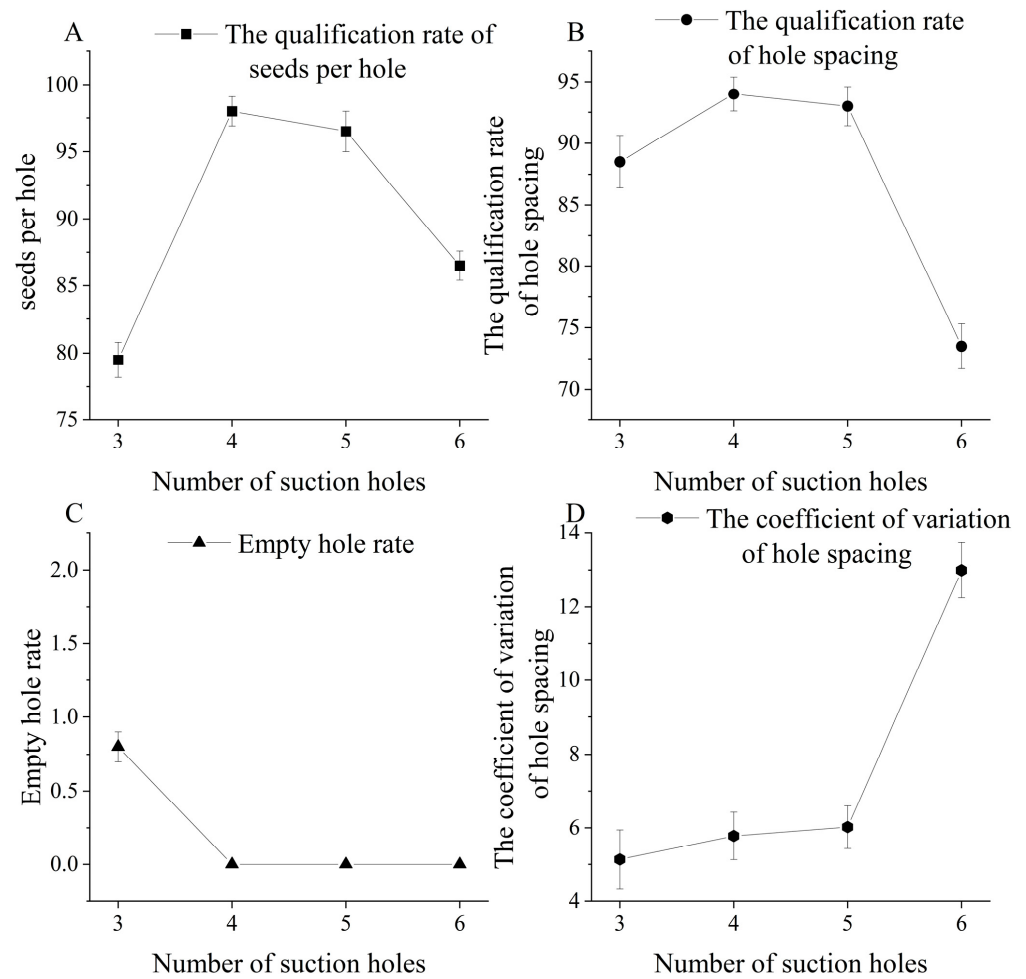3.2.1. Influence of Suction Hole Spacing on Sowing Performance

In single-factor experiments, varying suction hole spacing was the variable; the results are shown in Figure 16. The results indicate that when the spacing of the seed suction holes is at D3, the short spacing between the holes leads to a serious issue of multi-suction, resulting in a significant decrease in the rate of qualified hole grain numbers. As the spacing between the suction holes increases, the phenomenon of multi-suction gradually decreases, leading to a gradual improvement in the index of qualified hole grains. This indicates that the spacing between suction holes is a critical factor in ensuring the quality of seed sowing.
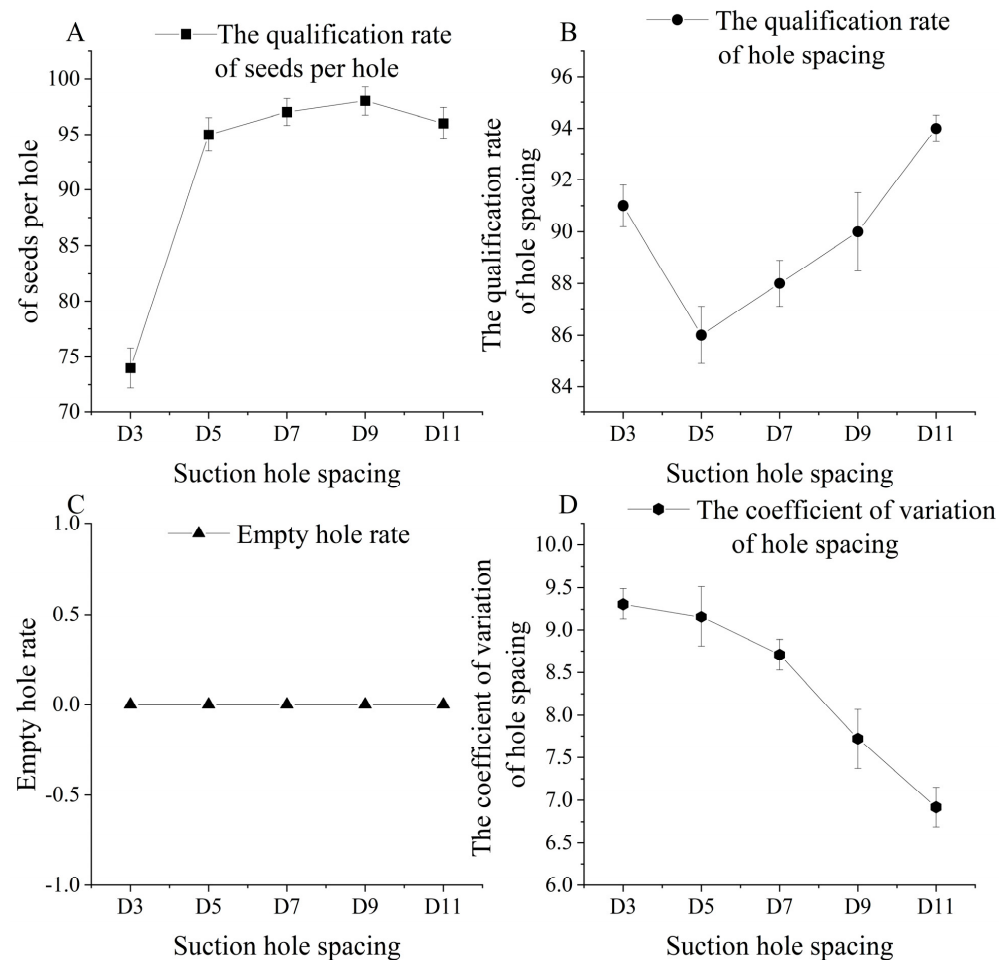
Figure 16. Influence of suction hole spacing on sowing performance. (**A**). The qualification rate of seeds per hole; (**B**). The qualification rate of hole spacing; (**C**). Empty hole rate; (**D**). The coefficient of variation of hole spacing.

3.2.2. Influence of Number of Suction Holes on Sowing Performance

The results of single-factor experiments varying the number of suction holes are shown in Figure 17. The results indicate that the performance is better when the number of suction holes is set to 4 or 5, with all evaluation indices tending to stabilize. When the number of holes is 3, there is a significant issue of missing suction, leading to a noticeable drop in the rate of qualified hole grain numbers. Conversely, with six holes, there is a serious problem of multi-suction, causing a significant decline in both the qualification rate of seeds per hole and the qualification rate of hole spacing.
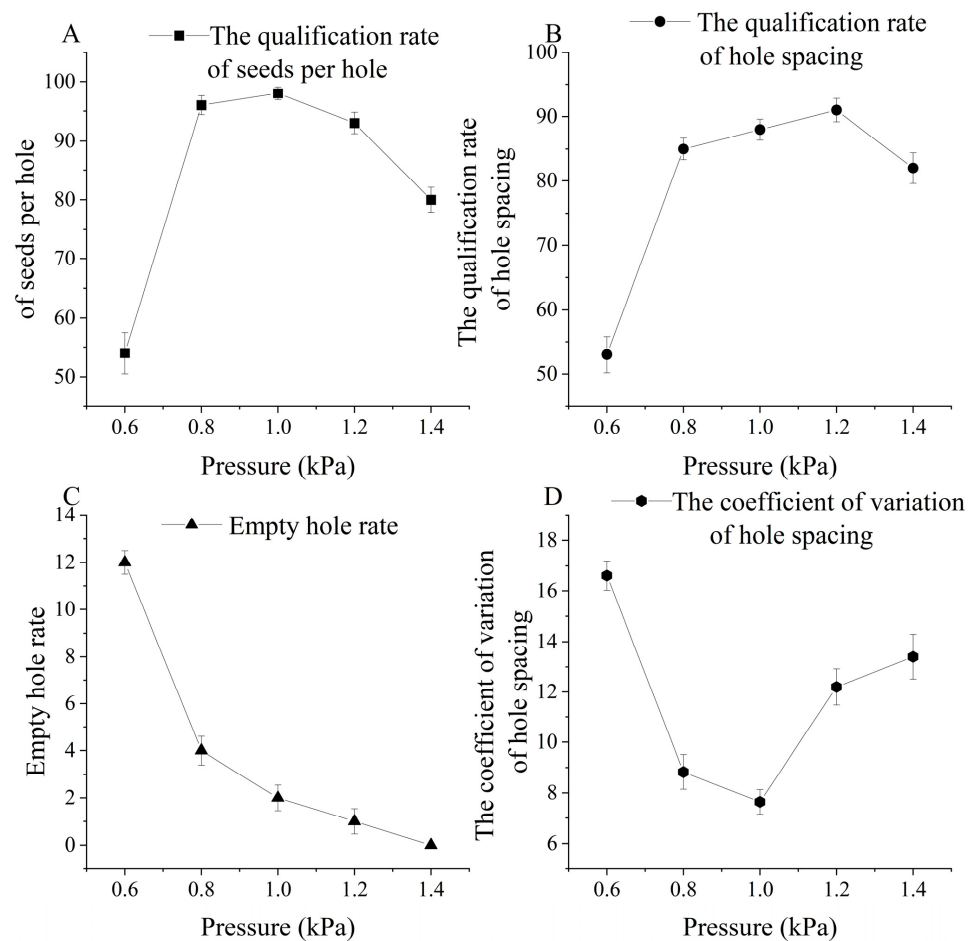
Figure 17. Influence of the number of suction holes on seed discharge performance. (**A**). The qualification rate of seeds per hole; (**B**). The qualification rate of hole spacing; (**C**). Empty hole rate; (**D**). The coefficient of variation of hole spacing.

3.2.3. Influence of Negative Pressure on Sowing Performance

The results of single-factor experiments varying the air chamber negative pressure as the variable are shown in Figure 18.

The results indicate that when the vacuum level in the air suction chamber is below −0.8 kPa, seeds cannot be stably suctioned, leading to serious missed sowing. This results in a lower qualification rate of seeds per hole and a higher empty hole rate. When the vacuum level in the air suction chamber is at −1.4 kPa, the phenomenon of multiple seeds being suctioned into one hole becomes more pronounced. Although within the range of qualified hole grain numbers, the qualification rate of seeds per hole fluctuates widely, resulting in poor sowing stability. As the vacuum level increases, the qualification rate of seeds per hole and the qualification rate of hole spacing initially rise and then decrease, with the empty holes rate gradually dropping to zero.

Figure 18. Influence of negative pressure on sowing performance. (**A**). The qualification rate of seeds per hole; (**B**). The qualification rate of hole spacing; (**C**). Empty hole rate; (**D**). The coefficient of variation of hole spacing.

3.3. Results Analysis of the Box–Behnken Test

3.3.1. Box–Behnken Test Results

During the response surface experiments, it was observed that the rate of empty holes met the agronomic requirements. Consequently, this study conducted response surface experiments using the qualification rate of seeds per hole, the qualification rate of hole spacing, and the hole spacing coefficient of variation as evaluation indicators. The test scheme and results are provided in Table 5.

Table 5. Experimental design and results.

Test Serial Number	Factors			Evaluation Indicators		
	A	B	C	The Qualification Rate of Seeds per Hole Y_1	The Qualification Rate of Hole Spacing Y_2	The Hole Spacing Coefficient of Variation Y_3
1	4	11	0.8	96	85	3.91
2	5	7	1	93.4	93	16.83
3	4	9	1	99.2	96.4	5.64
4	3	11	1	86	88.5	10.89
5	3	9	1.2	86.4	89	10.94
6	3	7	1	79.8	84.2	11.56
7	5	9	0.8	94.4	93	8.58

Table 5. *Cont.*

Test Serial Number	Factors			Evaluation Indicators		
	A	**B**	**C**	**The Qualification Rate of Seeds per Hole Y_1**	**The Qualification Rate of Hole Spacing Y_2**	**The Hole Spacing Coefficient of Variation Y_3**
8	4	9	1	98.4	94.8	5.84
9	5	9	1.2	85.8	86	13.48
10	3	9	0.8	76.2	81.8	10.94
11	4	9	1	97.8	95.2	5.24
12	4	9	1	98	94.2	6.64
13	4	7	0.8	96.2	89.6	8.71
14	4	9	1	98.8	95.8	5.94
15	4	11	1.2	97.8	91	6.24
16	5	11	1	90.4	90.8	7.86
17	4	7	1.2	93.6	82.6	11.2

3.3.2. Regression Equation ANOVA

Using Design-Expert 13 software for regression analysis of the experimental results, regression equations were obtained between Y_1 (The qualification rate of seeds per hole), Y_2 (The qualification rate of hole spacing), and Y_3 (The hole spacing coefficient of variation) and the variables A (Number of suction holes), B (suction hole spacings), and C (Negative pressures), as shown in (13).

$$\begin{cases} Y_1 = 98.79 + 3.3A + 0.24B + 0.65C - 1.15AB - 4.7AC + 0.55BC - 10.62A^2 - 0.105B^2 - 2.12C^2 \\ Y_2 = 94.83 + 1.60A - 1.27B + 1.53C - 0.8125AB - 3.55AC + 1.63BC - 2.88A^2 - 0.8194B^2 - 4.95C^2 \\ Y_3 = 4.95 - 0.735A - 0.5988B + 1.2C - 1.04AB + 1.23AC - 0.02BC + 4.7A^2 + 0.3069B^2 + 0.4275C^2 \end{cases} \quad (13)$$

According to the analysis of variance results (as shown in Table 6), the model terms for Y_1 (The qualification rate of seeds per hole), Y_2 (The qualification rate of hole spacing), and Y_3 (The hole spacing coefficient of variation) were all highly significant, while the lack-of-fit terms were not significant. This indicates that the regression equations can fit the actual situation well. The determination coefficients (R^2) for Y_1, Y_2, and Y_3 are 0.997, 0.987, and 0.992, respectively, with Adequacy Precision values all greater than 4. This suggests that the model can be effectively used to navigate the design space. By excluding non-significant influencing factors, the refined regression equations were obtained, as shown in (14).

$$\begin{cases} Y_1 = 98.79 + 3.3A + 0.65C - 1.15AB - 4.7AC + 0.55BC - 10.62A^2 - 2.12C^2 \\ Y_2 = 94.83 + 1.60A - 1.27B + 1.53C - 0.8125AB - 3.55AC + 1.63BC - 2.88A^2 - 0.8194B^2 - 4.95C^2 \\ Y_3 = 4.95 - 0.735A - 0.5988B + 1.2C - 1.04AB + 1.23AC + 4.7A^2 + 0.3069B^2 \end{cases} \quad (14)$$

Table 6. ANOVA results.

Source	Y_1		Y_2		Y_3	
	F	**P**	**F**	**P**	**F**	**P**
Model	288.17	**	61.5	**	92.16	**
A	190.69	**	21.14	**	12.76	**
B	2.09	0.19	27.56	**	17.51	**
C	7.4	**	19.21	**	33.72	*
AB	69.47	**	16.36	**	76.25	**
AC	290.11	**	78.06	**	26.58	**
BC	15.89	**	65.42	**	0.0283	0.87
A^2	1559.18	**	53.99	**	411.36	**
B^2	2.44	0.16	70.04	**	28.09	**
C^2	62.13	**	159.92	**	3.41	0.10
Lock of fit	0.8333	0.54	0.7252	0.59	0.6782	0.61

Note: * indicates significant difference ($0.01 \leq p < 0.05$); ** indicates highly significant difference ($p < 0.05$).
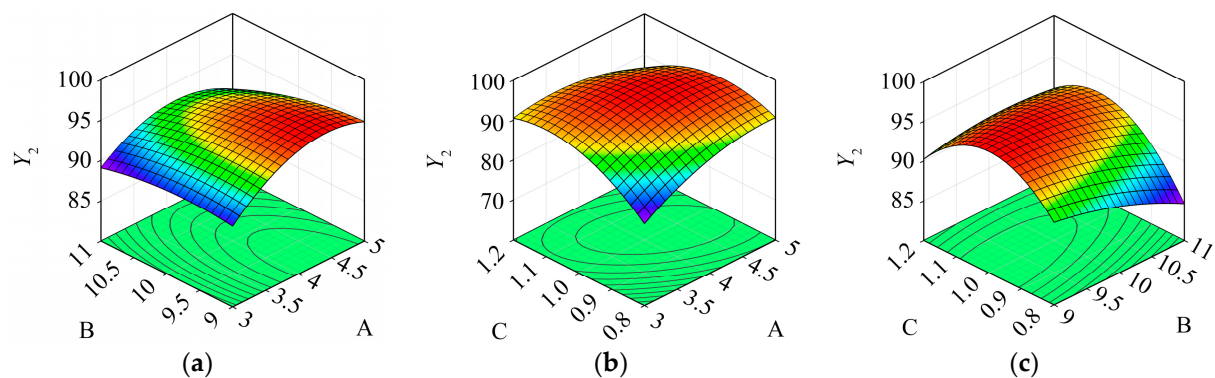
3.3.3. Significant Interaction Analysis

As shown in Figure 19, the interactions between the number of suction holes, their positions, and the negative pressure significantly affect the qualification rate of seeds per hole. When the position of the suction holes is fixed, the qualification rate of seeds per hole initially increases and then decreases with the rise in the number of suction holes and negative pressure. When there are three suction holes, the qualification rate of seeds per hole tends to decrease with increasing negative pressure. Conversely, when there are five suction holes, the qualification rate of seeds per hole tends to increase with increasing negative pressure. When the negative pressure is fixed, the qualification rate of seeds per hole initially increases and then decreases as the number of suction holes increases.
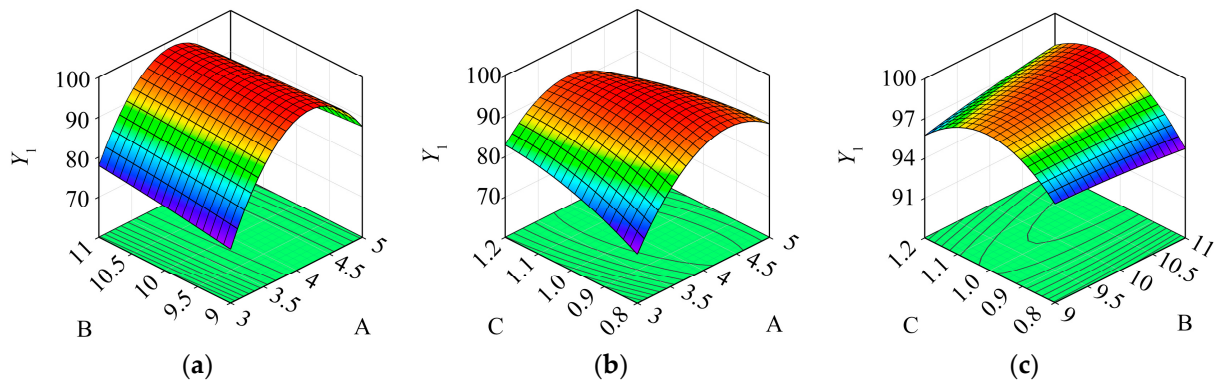
Figure 19. The impacts of interaction factors on the qualification rate of seeds per hole. (**a**). AB interaction; (**b**). AC interaction; (**c**). BC interaction.

As illustrated in Figure 20, the interactions between the number of suction holes, their positions, and the negative pressure also significantly influence the qualification rate of hole spacing. With a fixed suction hole spacing, the qualification rate of hole spacing shows an initial increase followed by a decrease with an increase in the number of suction holes and negative pressure. When the number of suction holes is fixed, the qualification rate of hole spacing first increases and then decreases as the negative pressure rises. When the negative pressure is fixed, the qualification rate of hole spacing initially increases and then decreases with the number of suction holes. At a negative pressure of 0.8, the qualification rate of hole spacing gradually declines with increasing suction hole spacing; at a negative pressure of 1.2, it tends to rise with the suction hole spacing.

Figure 20. The impacts of interaction factors on the qualification rate of hole spacing. (**a**). AB interaction; (**b**). AC interaction; (**c**). BC interaction.

As illustrated in Figure 21, the interactions between the number of suction holes and their positions, as well as the number of suction holes and negative pressure, have a significant effect on the hole spacing coefficient of variation. With a fixed suction hole

spacing, the hole spacing coefficient of variation first decreases and then increases with the number of suction holes. When there are three suction holes, the hole spacing coefficient of variation increases with the position of the suction holes; when there are five suction holes, it decreases with the position of the suction holes. With a fixed negative pressure, the hole spacing coefficient of variation first decreases and then increases as the number of suction holes increases.
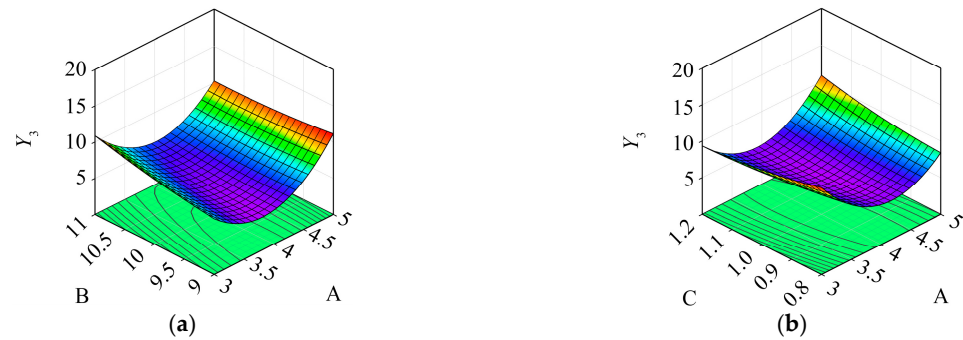
Figure 21. The impacts of interaction factors on coefficient of variation of hole spacing. (**a**). AB interaction; (**b**). BC interaction.

3.4. Verification Test

Using Design-Expert software to determine the optimal combination of working parameters, we set constraints such that the qualification rate of seeds per hole and the qualification rate of hole spacing should be maximized while the hole spacing coefficient of variation should be minimized. The prediction is that when the number of suction holes is set to 4.18, suction hole spacings to 9.7, and negative pressure to 0.99, the qualification rate of seeds per hole, the qualification rate of hole spacing, and the hole spacing coefficient of variation would be 99.09%, 95.27%, and 5.08%, respectively. Benchtop experiments were conducted to verify these predictions. Considering that the predicted results do not conform to actual production and processing conditions, they were rounded to whole numbers. Therefore, the number of suction holes was set to 4, suction hole spacings to 10, and negative pressure to 1, and three repeated experiments were conducted. The experimental results are shown in Table 7, with the qualification rate of seeds per hole, the qualification rate of hole spacing, and the hole spacing coefficient of variation being 98.67%, 96%, and 5.24%, respectively, meeting agronomic standards.

Table 7. Validation test results.

Number	Y_1	Y_2	Y_3
1	99	94	6.84
2	98	98	4.28
3	99	96	4.61
Average value	98.67	96	5.24

4. Discussion

This paper further investigates the influence of the cluster hole effect on the multi-seed precision sowing performance of quinoa seeds, utilizing the CFD method to analyze the impact of different suction hole spacing, numbers, and suction negative pressure on the suction area. Through single-factor experiments, the key factors affecting the cluster hole effect were identified. To avoid the decline in multi-seed precision sowing stability caused by the cluster hole effect, based on the results of the Box–Behnken (BB) experiments, the interaction effects of significant factors on the cluster hole effect were analyzed, and optimal parameter combinations were clarified. The detailed discussion is as follows:

(1) The spacing between suction holes significantly affects the suction range and airflow velocity. When the spacing between the seed suction holes is close, the airflow velocity changes more rapidly. The airflow between two suction holes affects each other, leading to an increase in velocity and suction area at the suction holes and the possibility of seeds being adsorbed between the holes (Figure 10). When the suction hole spacing is less than 5 mm, the cluster hole effect is obvious. Multiple seeds are still adsorbed between the suction holes (Figure 16).

(2) The number of suction holes has a minor impact on the flow field (Figure 13). However, having too few or too many holes can decrease the qualification rate of seeds per hole, so a number of 4 or 5 holes is more appropriate (Figure 17). The number of holes mainly affects the negative pressure and, thereby, the suction area. As the area of the suction holes increases, the negative pressure gradually decreases, and the velocity at the holes gradually reduces.

(3) Negative pressure significantly affects both the suction range and airflow velocity (Figure 15). When the negative pressure is too low, even if seeds occupy favorable suction positions, stable suction conditions cannot be achieved, leading to an increase in the rate of empty holes (Figure 18); when the negative pressure is too high, the effective suction range of seeds increases, a single seed cannot occupy the entire effective suction area, and diffusive airflow can still stably adsorb seeds, causing a decrease in the rate of qualified grains per hole (Figure 18). This is consistent with previous research on the impact of negative pressure on sowing performance.

(4) The interaction between suction hole spacing, number, and negative pressure has a significant impact on evaluation indicators (Table 6). The interaction between hole spacing and number increases the number of collisions during the seeding process, leading to a decrease in the qualification rate of hole spacing and an increase in the hole spacing coefficient of variation. The interaction between hole spacing and negative pressure causes too much variation in seeding positions, leading to decreased performance of the seed metering device. When the negative pressure is low, and the number of holes is limited, seed suction becomes unstable, leading to an increased likelihood of missed seeding. Conversely, at higher negative pressures and with a greater number of holes, seed suction stabilizes, but it results in a higher incidence of duplicate seeding.

(5) In the multi-seed precision sowing process of small-diameter crops, it is necessary to avoid the cluster hole effect as much as possible. However, if the combination of suction hole spacing, size, and negative pressure is well-managed, the cluster hole effect can produce a stable suction flow field, prevent large-diameter seeds from getting stuck in the holes, and thereby improve the performance of air-suction seed metering devices for large-diameter seeds.

5. Conclusions

(1) Based on theoretical analysis and CFD simulation results, it is found that the cluster hole effect is influenced by various factors, including the diameter and spacing of suction holes, seed shape, and pressure gradient difference. Specifically, the spacing between suction holes and the pressure gradient significantly affect the cluster hole effect.

(2) Single-factor experiment results show that seed discharge performance is significantly affected by the negative pressure in the air chamber, the spacing between suction holes, and the number of suction holes. Optimal seed discharge performance is achieved when the air chamber negative pressure is 0.8–1.2 kPa, the suction hole spacing is between 7 and 9 mm, and the number of suction holes is 3–5.

(3) Through the Box–Behnken response surface experiment, taking negative pressure, spacing between suction holes, and the number of suction holes as factors, the optimal parameter configuration was determined. Validation experiments confirmed that when the number of seed suction holes is four, the distribution spacing of the seed

suction holes is at D10, and the vacuum degree is 1 kPa, the performance is optimal, achieving a 98.67% qualified rate of seeds per hole, 96% qualified rate of hole spacing, and a 5.24 coefficient of variation for hole spacing, meeting agronomic requirements.

References

1. Hu, H.Y.; Shao, T.Y.; Gao, X.M.; Long, X.H.; Rengel, Z. Effects of planting quinoa on soil properties and microbiome in saline soil. *Land Degrad. Dev.* **2022**, *33*, 2689–2698. [CrossRef]
2. Chaudhary, N.; Walia, S.; Kumar, R. Functional composition, physiological effect and agronomy of future food quinoa (*Chenopodium quinoa* Willd.): A review. *J. Food Compos. Anal.* **2023**, *118*, 105192. [CrossRef]
3. Shi, L.R.; Zhao, W.Y.; Sun, B.G.; Sun, W.; Zhou, G. Determination and analysis of basic physical and contact mechanics parameters of quinoa seeds by DEM. *Int. J. Agric. Biol. Eng.* **2023**, *16*, 35–43. [CrossRef]
4. Zheng, J.; Liao, Y.T.; Liao, Q.X.; Sun, M. Trend analysis and prospects of seed metering technologies. *Trans. Chin. Soc. Agric. Eng.* **2022**, *38*, 1–13. [CrossRef]
5. Yuan, Y.W.; Bai, S.H.; Niu, K.; Zhou, L.M.; Zhao, B.; Wei, L.G.; Liu, L.J. Research progress in the key technologies and equipment for cotton planting mechanization. *Trans. Chin. Soc. Agric. Eng.* **2023**, *39*, 1–11. [CrossRef]
6. Du, Z.H.; He, X.T.; Yang, L.; Zhang, D.X.; Cui, T.; Zhong, X.J. Research progress on precision variable-rate seeding technology and equipment for maize. *Trans. Chin. Soc. Agric. Eng.* **2023**, *39*, 1–16. [CrossRef]
7. Li, H.Q.; Zhao, C.J.; Yan, B.X.; Ling, L.; Meng, Z.J. Design and Verification of the Variable Capacity Roller-Wheel Precision Rice Direct Seed-Metering Device. *Agronomy* **2022**, *12*, 1798. [CrossRef]
8. Guo, H.P.; Cao, Y.Z.; Song, W.Y.; Zhang, J.; Wang, C.L.; Wang, C.S.; Yang, F.Z.; Zhu, L. Design and Simulation of a Garlic Seed Metering Mechanism. *Agriculture* **2021**, *11*, 1239. [CrossRef]
9. Xu, J.; Hou, J.W.; Wu, W.B.; Han, C.Y.; Wang, X.M.; Tang, T.; Sun, S.L. Key Structure Design and Experiment of Air-Suction Vegetable Seed-Metering Device. *Agronomy* **2022**, *12*, 675. [CrossRef]
10. Ding, Y.C.; Wang, K.Y.; Liu, X.D.; Liu, W.P.; Chen, L.Y.; Liu, W.B.; Du, C.Q. Research progress of seeding detection technology for medium and small size seeds. *Trans. Chin. Soc. Agric. Eng.* **2021**, *37*, 30–41. [CrossRef]
11. Shi, B.B.; Zhang, J.; Wang, L.; Liao, Q.X.; Liao, Y.T. Design and Experiment of Pneumatic Adaptive Seeding System for Small Particle Size Seeds. *Trans. Chin. Soc. Agric. Mach.* **2023**, *54*, 30–41. [CrossRef]
12. Tang, H.; Guan, T.Y.; Xu, F.D.; Xu, C.S.; Wang, J.W. Test on suction posture and seeding performance of the high-speed precision dual-chamber maize metering device based on the seed characteristics. *Comput. Electron. Agric.* **2024**, *216*, 108471. [CrossRef]
13. Li, C.; Cui, T.; Zhang, D.X.; Yang, L.; He, X.T.; Li, Z.M.; Jing, M.S.; Dong, J.Q.; Xing, S.L. Design and experiment of a centrifugal filling and cleaning high-speed precision seed metering device for maize. *J. Clean. Prod.* **2023**, *426*, 139083. [CrossRef]
14. Karayel, D.; Güngör, O.; Šarauskis, E. Estimation of Optimum Vacuum Pressure of Air-Suction Seed-Metering Device of Precision Seeders Using Artificial Neural Network Models. *Agronomy* **2022**, *12*, 1600. [CrossRef]
15. Xia, Q.Q.; Zhang, W.Y.; Qi, B.; Wang, Y.X. Design and Experimental Study on a New Horizontal Rotary Precision Seed Metering Device for Hybrid Rice. *Agriculture* **2023**, *13*, 158. [CrossRef]
16. Zhao, X.; Zhang, T.; Liu, F.; Li, N.; Li, J.R. Sunflower Seed Suction Stability Regulation and Seeding Performance Experiments. *Agronomy* **2022**, *13*, 54. [CrossRef]
17. Zhao, X.S.; Ran, W.J.; Hao, J.J.; Bai, W.J.; Yang, X.L. Design and experiment of the double-seed hole seeding precision seed metering device for peanuts. *Int. J. Agric. Biol. Eng.* **2022**, *15*, 107–114. [CrossRef]
18. Qiao, X.D.; Liu, D.Q.; Wang, X.L.; Wang, L.; Wang, J.W.; Zheng, D.C. Design and Experiment of Double-Row Seed-Metering Device for Buckwheat Large Ridges. *Agriculture* **2023**, *13*, 1953. [CrossRef]

19. Gao, X.J.; Xie, G.F.; Li, J.; Shi, G.S.; Lai, Q.H.; Huang, Y.X. Design and validation of a centrifugal variable-diameter pneumatic high-speed precision seed-metering device for maize. *Biosyst. Eng.* **2023**, *227*, 161–181. [CrossRef]

20. Liu, R.; Liu, Z.J.; Zhao, J.L.; Lu, Q.; Liu, L.J.; Li, Y.H. Optimization and Experiment of a Disturbance-Assisted Seed Filling High-Speed Vacuum Seed-Metering Device Based on DEM-CFD. *Agriculture* **2022**, *12*, 1304. [CrossRef]

21. Tang, H.; Xu, C.S.; Guo, F.Y.; Yao, Z.G.; Jiang, Y.M.; Guan, R.; Sun, X.B.; Wang, J.W. Analysis and Experiment on the Seed Metering Mechanism of Multi-Grain Cluster Air Suction Type Rice (*Oryza sativa* L.) Hill Direct Seed Metering Device. *Agriculture* **2022**, *12*, 1094. [CrossRef]

22. Li, D.P.; Lui, F.; Zhao, M.Q.; Yue, Y.; Zhang, T.; Lin, Z. Structural desin and performance test of one pneumatic millet precision seed metering device. *J. China Agric. Univ.* **2019**, *24*, 141–151. [CrossRef]

23. Liao, Y.T.; Liao, Q.X.; Wang, L.; Zheng, J.; Gao, L.P. Investigation on vacuum singulating effect influencing factors of pneumatic precision seed metering device for small particle size of seeds. *Trans. Chin. Soc. Agric. Eng.* **2018**, *34*, 10–17. [CrossRef]

24. Li, Z.D.; He, S.; Zhong, J.Y.; Han, J.F.; Chen, Y.X.; Song, Y. Parameter optimization and experiment of the disturbance pneumatic plate hole metering device for rapeseed. *Trans. Chin. Soc. Agric. Eng.* **2021**, *37*, 1–11. [CrossRef]

25. Li, B.H.; Ahmad, R.; Qi, X.D.; Li, H.; Nyambura, S.M.; Wang, J.F.; Chen, X.; Li, S.B. Design Evaluation and Performance Analysis of a Double-Row Pneumatic Precision Metering Device for Brassica chinensis. *Sustainability* **2021**, *13*, 1374. [CrossRef]

26. Xu, J.; Sun, S.L.; He, Z.K.; Wang, X.M.; Zeng, Z.H.; Li, J.; Wu, W.B. Design and optimisation of seed-metering plate of air-suction vegetable seed-metering device based on DEM-CFD. *Biosyst. Eng.* **2023**, *230*, 277–300. [CrossRef]

27. Popov, A.Y.; Muratov, D.K. Study of the sealing elements impact on air flow distribution in a seed vessel of seeding mechanism. *MATEC Web Conf.* **2018**, *224*, 05015. [CrossRef]

28. Wang, N.; Wang, F.X.; Shock, C.C.; Meng, C.B.; Qiao, L.F. Effects of Management Practices on Quinoa Growth, Seed Yield, and Quality. *Agronomy* **2020**, *10*, 445. [CrossRef]

29. Zulkadir, G.; İdikut, L. The impact of various sowing applications on the nutritional value of Quinoa Dry Herb. *J. Food Process. Preserv.* **2021**, *45*, e15730. [CrossRef]

30. Liu, W.Z.; Zhao, M.Q.; Wang, W.M.; Zhao, S.J. Theoretical analysis and experiments of metering performance of the pheumatic seed metering device. *Trans. Chin. Soc. Agric. Eng.* **2010**, *26*, 133–138. [CrossRef]

31. Wang, Y.J.; Su, W.; Lai, Q.H.; Lin, Y.H.; Li, J.H. Simulation and measurement of the suction force on ellipsoidal seeds in an air-suction seed-metering device. *Biosyst. Eng.* **2023**, *232*, 97–113. [CrossRef]

32. Li, J.H.; Lai, Q.H.; Zhang, H.; Zhang, Z.G.; Zhao, J.W.; Wang, T.T. Suction force on high-sphericity seeds in an air-suction seed-metering device. *Biosyst. Eng.* **2021**, *211*, 125–140. [CrossRef]

33. Guarella, P.; Pellerano, A.; Pascuzzi, S. Experimental and theoretical performance of a vacuum seeder nozzle for vegetable seeds. *J. Agric. Eng. Res.* **1996**, *64*, 29–36. [CrossRef]

34. Wang, L.; Cong, J.L.; Ren, N.; Ying, J.C.; Wang, X.D.; Liao, Y.T.; Liao, Q.X. Influence of surface slope on the seeding performance of air-assisted centralized metering device for rapeseed based on numerical simulation. *Comput. Electron. Agric.* **2024**, *218*, 108734. [CrossRef]